Chemical Science

ROYAL SOCIETY
OF CHEMISTRY

15 YEARS ANNIVERSARY

EDGE ARTICLE
Dillip Kumar Chand *et al.*
Hosting of [Cs(crown ether)$_2$]$^+$ type host–guest complexes
by a nano-sized molecular cuboid

Hosting of [Cs(crown ether)₂]⁺ type host–guest complexes by a nano-sized molecular cuboid

Manaswini Ray, Shobhana Krishnaswamy [ID] and Dillip Kumar Chand [ID] *

Encapsulation of a guest by host-forming (G-in-H)-type host–guest complexes is the central theme of supramolecular chemistry. Binding of typical hosts (H_{in}) in the cavity of a larger host (H_{out}) to form (H_{in}-in-H_{out}) type assemblies is also known. However, the incorporation of host–guest complexes in a larger host to form [(G-in-H_{in})-in-H_{out}] type assemblies, where (G-in-H_{in}) is composed of one guest and one host is relatively unexplored. A recent report describes the binding of host–guest complexes consisting of one guest and two hosts in a larger host molecule. In the present work, we have prepared a nano-sized polycationic molecular cuboid of the type $Pd(L')_8(L)_4$ as the H_{out}, which is capable of encapsulating two units of H_{in} such as dibenzo[3n]crown-n (where n ranges from 6 to 8). The molecular cuboid is found to selectively recognize the larger-sized dibenzo[24]crown-8 and dibenzo[21]crown-7 over the smaller-sized dibenzo[18]crown-6. The polycationic molecular cuboid can bind a family of [Cs(crown ether)₂]⁺ type cationic host–guest complexes composed of one unit of a guest (Cs⁺) and two units of the H_{in} (crown ether). All these complexes are prepared *via* self-assembly in a water medium; the surrogate nuclear waste Cs⁺ is deeply internalized, being encapsulated by two units of crown ether, which are in turn sheltered by the molecular cuboid. All the [G-in-(H_{in})₂-in-H_{out}] type assemblies are characterized using spectroscopic techniques and single-crystal structures. The relative orientation of the pair of crown ethers around the Cs⁺ ion is found to be different in the native form compared to the encapsulated form in the molecular cuboid.

1 Introduction

Host–guest chemistry is a well acknowledged central theme of supramolecular chemistry that many researchers have pursued intensely, employing a variety of host and guest entities to achieve intriguing results.[1–7] Host–guest complexes composed of one variety of host and one variety of guest can be formulated as $[(G)_x \subset (H)_y]$ where the values of x and y are variable but small, the simplest varieties being $[(G) \subset (H)]$, $[(G)_2 \subset (H)]$ and $[(G) \subset (H)_2]$.[4,8,9] A smaller host molecule may behave like a guest molecule when one or more units of the host are accommodated in the cavity of a larger host molecule to form host-in-host type complexes. The molecular recognition of a host, H_{in}, by another host, H_{out}, is relatively less studied; such host-in-host species can be formulated as $[(H_{in})_y \subset (H_{out})]$ where $y \geq 1$. The larger host, *i.e.*, H_{out}, could be a coordination cage or a covalent cage entity.[10–16] If H_{in} comes in contact with a complementary guest molecule G either (i) prior to binding with H_{out}, (ii) during binding with H_{out}, or (iii) after binding with H_{out}, then the combined interactions among G, H_{in} and H_{out} should result in higher-order structures such as $[\{(G)_x \subset (H_{in})_y\}_z \subset (H_{out})]$. Encapsulation of one unit of $[(G) \subset (H_{in})]$ in the cavity of H_{out} to

form a $[\{(G) \subset (H_{in})\} \subset (H_{out})]$ type super-assembly (where $x = 1$, $y = 1$ and $z = 1$) is known.[17–29] Additionally, there is an example of the encapsulation of two units of $[(G) \subset (H_{in})]$ in the nanospace of H_{out} to give a $[\{(G) \subset (H_{in})\}_2 \subset (H_{out})]$ type assembly (where $x = 1$, $y = 1$ and $z = 2$).[30] A very recent report by Fujita demonstrated the assembly of G, H_{in} and H_{out} in which the guest molecule G is sandwiched by two units of H_{in} to form a $[(G) \subset (H_{in})_2]$ type entity located inside the cavity of H_{out}, giving rise to a series of elaborate $[\{(G) \subset (H_{in})_2\} \subset (H_{out})]$ type molecules (where $x = 1$, $y = 2$ and $z = 1$).[31] The encapsulation of either a suitable host or host–guest entity *via* molecular confinement in another larger host is relatively underexplored. Such phenomena are worthy of investigation as they are anticipated to provide novel supramolecular behaviours including the stabilization of otherwise unstable species, the imposition of unusual conformations and novel behaviours on the bound species, the modulation of guest binding strength/selectivity, unusual product formation *via* catalysis reactions in the confined space, *etc.*

In the present work, we disclose the preparation of $[(H_{in})_2 \subset (H_{out})]$ and $[\{(G) \subset (H_{in})_2\} \subset (H_{out})]$ type super-assemblies in a water medium using the same G and H_{out} units with different H_{in} as shown in Fig. 1. The outer-host, *i.e.*, H_{out}, explored here is a new cuboid-shaped self-assembled nanosized coordination cage with the formula $[Pd_8(L')_8(L)_4]^{16+}$, where L′ represents tetramethylethylenediamine (tmeda) and L

IoE Center of Molecular Architecture, Department of Chemistry, Indian Institute of Technology Madras, Chennai 600036, India. E-mail: dillip@zmail.iitm.ac.in
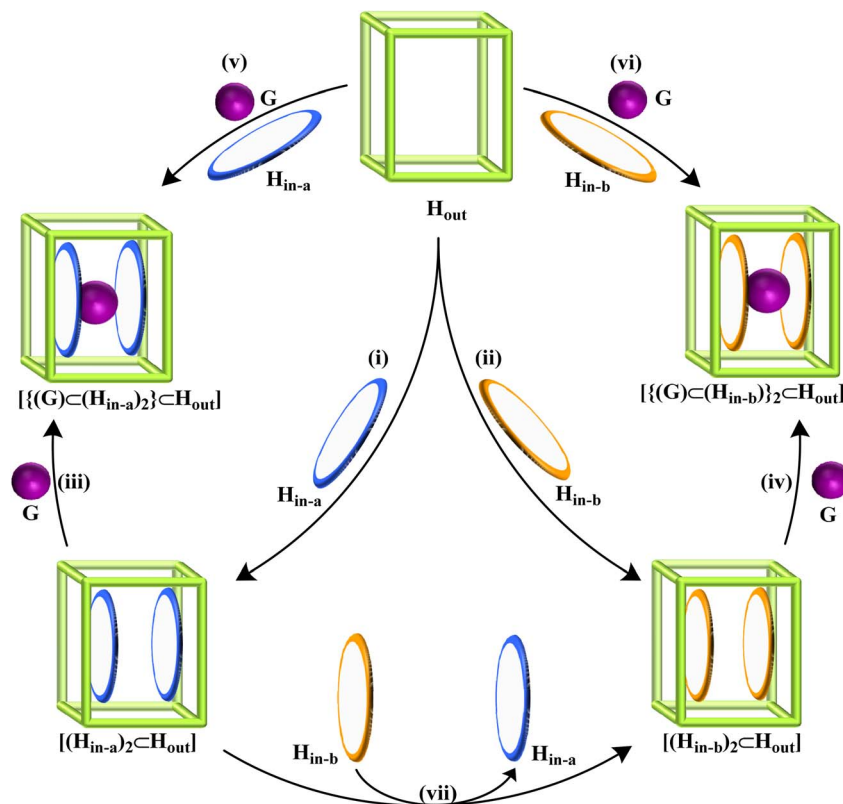
Fig. 1 Conceptualizing the synthesis of assemblies of (i and ii) $[(H_{in})_2 \subset (H_{out})]$ and (iii–vi) $[\{(G) \subset (H_{in})_2\} \subset (H_{out})]$ type molecules. (vii) H_{in} exchange reaction showing selective inclusion of one type of H_{in} over another type of H_{in} by H_{out}.

is a rectangular panel-shaped 4-pyridyl appended tetrakis monodentate ligand. The family of inner-hosts, $i.e.$, H_{in}, used in this study includes a range of classical crown ethers such as dibenzo[$3n$]crown-n (n = 6, 7, and 8), and a surrogate nuclear waste, namely, Cs^+, is used as the cationic guest G. For the $[(H_{in})_2 \subset (H_{out})]$ type assemblies, the selective binding of one type of H_{in} ($e.g.$, dibenzo[24]crown-8 or dibenzo[21]crown-7) over the binding of another H_{in} ($i.e.$, dibenzo[18]crown-6) by the outer host H_{out} is observed. The relative orientations of the two crown ether units in the structure of $[(Cs)(crown ether)_2]^+$ in the native state and encapsulated state (in the cavity of H_{out}) showed remarkable differences.

2 Results and discussion

2.1 Conceptualization

The key objective of this work is to accomplish $[\{(G) \subset (H_{in})_2\} \subset (H_{out})]$ type water soluble molecules in a modular fashion by choosing a suitable set of G, H_{in} and H_{out}, as shown in Fig. 1. Self-assembled polycationic coordination cages having a nano-space could be ideal H_{out} type units, in view of the proven ability of such cages to encapsulate large-sized hydrophobic guest molecules.[32–35] The choice of H_{out} should be made on the basis of the overall shape and size of H_{in} or $vice\ versa$. Crown ethers such as dibenzo[$3n$]crown-n are macro-monocyclic hydrophobic host molecules are well known to accommodate alkali metal ions as guests. It should be possible to encapsulate

a typical crown ether like dibenzo[18]crown-6 in the cavity of a suitably designed coordination cage H_{out}. The flexible poly-ether chain of the crown ether can undergo conformational changes, if necessary, to become encapsulated in the available inner space of H_{out}. Thus, crown ethers, which themselves are typical hosts, may act as guests in a suitably designed large coordination cage (Fig. 1(i) and (ii)). In the encapsulated form, the crown ether may retain its initial ability to encapsulate a suitable alkali metal ion (Fig. 1(iii) and (iv)). In that case, the crown ether would play dual roles as both host and guest. For convenience, we herein use the term H_{in} for the crown ether (and H_{in-a} and H_{in-b} to distinguish two different crown ethers). The Cs^+ ion is larger than the cavity of dibenzo[18]crown-6; thus, it perches upon the crown ether cavity. For efficient binding, two units of this crown ether are required to sandwich one unit of Cs^+, forming $[(Cs) \subset (dibenzo[18]crown-6)_2]^+$, for which crystal structures have been reported. The design prin-ciple of the current work revolves around the use of a self-assembled coordination cage as H_{out}, typical crown ethers as H_{in}, and Cs^+ as the guest.

We are involved in the synthesis of Pd(II)-based self-assembled coordination cages using pyridine-appended multi-dentate ligands.[36] In a recent study, we combined a di-cationic cis-protected Pd(II), $i.e.$, (PdL′), and a rectangular panel-shaped 3-pyridyl appended tetrakis-monodentate ligand to prepare a self-assembled dodeca-cationic molecular prism of the type $Pd_6(L′)_6(L)_3$ that is capable of encapsulating small hydrophobic

guest molecules (neutral/polar/anionic) in a water medium.[37] In the current work, the complexation of *cis*-protected Pd(II) with a 4-pyridyl appended tetrakis monodentate ligand is undertaken in order to expand the cavity size to prepare a new molecular cuboid of the type $Pd_8(L')_8(L)_4$ for the encapsulation of larger-sized hydrophobic molecules in a water medium.

2.2 Nano-sized self-assembled molecular cuboid: H_{out}-type super-host

The tetrakis monodentate ligand 3,3′,5,5′-tetra(pyridin-4-yl)-1,1′-biphenyl, **L** (Fig. 2), which has a biphenyl core and four units of terminal 4-pyridyl rings on the periphery, was synthesized *via* a Suzuki–Miyaura cross-coupling reaction following a literature procedure.[38] Both the length and width of the panel-shaped rectangular ligand are greater than one nanometre. Surprisingly, the potential of this simple ligand for complexation with metal ions has not been explored to date. Complexation of *cis*-protected Pd(II) with the ligand **L** under optimized conditions produced the new molecular cuboids [Pd8(tmeda)8(**L**)4](NO3)16, **H1·16NO3**; [Pd8(tmeda)8(**L**)4](PF6)16, **H1·16PF6**; and [Pd8(en)8(**L**)4](NO3)16, **H2·16NO3** (Fig. 2), as described in this section.

Initially, a mixture of a slight excess of *cis*-Pd(tmeda)(NO3)2 (0.015 mmol) and the ligand **L** (0.005 mmol) was taken in 1 mL of D2O and stirred at room temperature, whereupon the metal component dissolved immediately and the ligand remained suspended even after 2 days of stirring. However, upon stirring
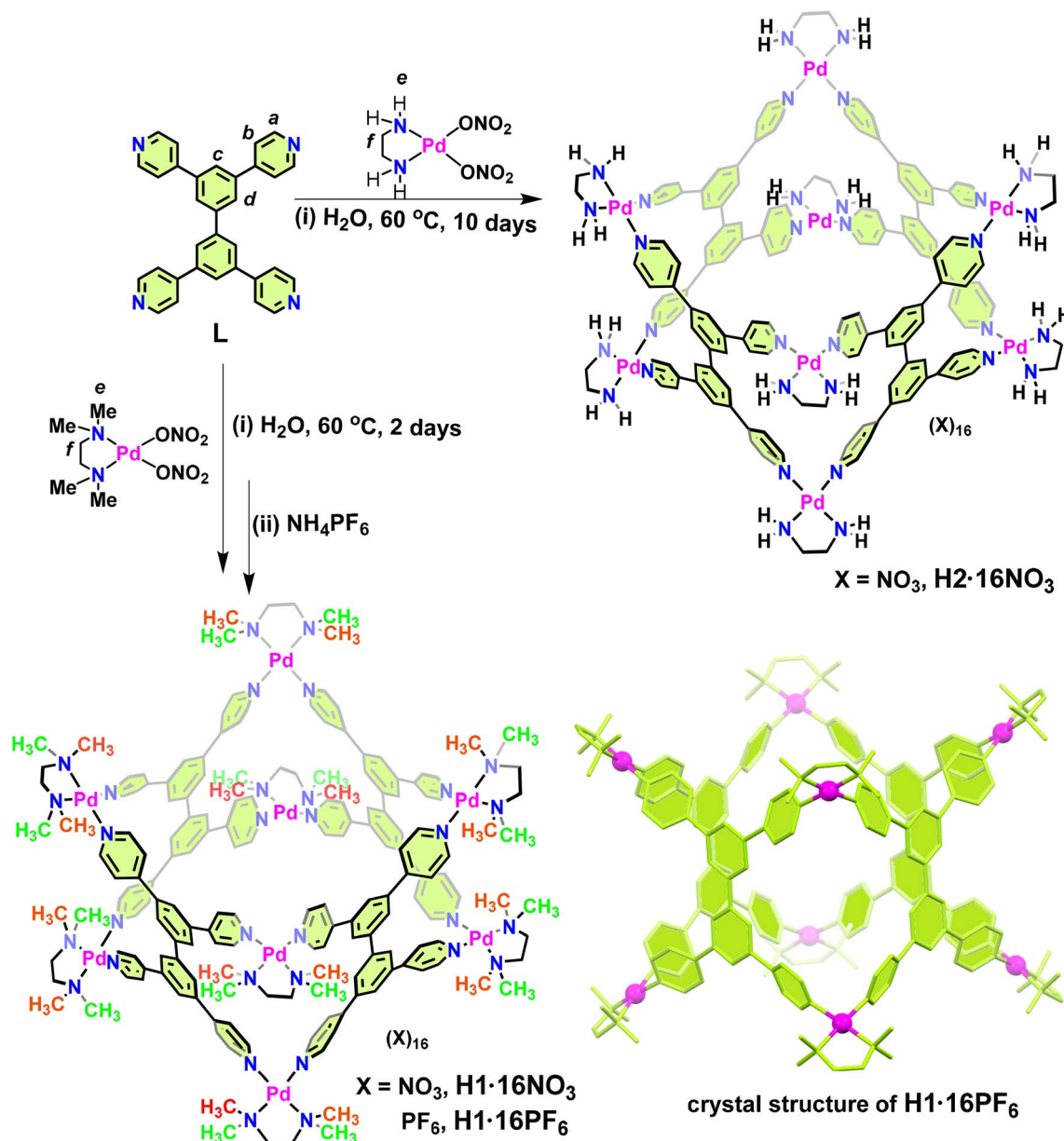

Fig. 2 Synthesis of the polycationic molecular cuboids [Pd8(tmeda)8(**L**)4](X)16 (X = NO3: **H1·16NO3**; X = PF6: **H1·16PF6**), and [Pd8(en)8(**L**)4](NO3)16, **H2·16NO3**. Crystal structure of **H1·16PF6** showing the [Pd8(tmeda)8(**L**)4]16+ architecture (counter anions and H atoms are not shown for clarity).

at 60 °C, the ligand was solubilized within 2 days. The reaction mixture was then cooled and centrifuged, and the supernatant containing the product was separated. The ^{1}H NMR spectrum of the *in situ* prepared sample (D$_2$O, 298 K, *i.e.*, 25 °C) showed a single set of slightly broad peaks (SI Fig. S11) along with signals corresponding to the unutilized metal component, indicating the formation of a single discrete coordination cage as the product. A mixed solvent such as H$_2$O : CH$_3$CN could lower the time required for the complexation reaction in this work, as already established by us for a related cage molecule. Thus, the complexation reaction was carried out in D$_2$O : CD$_3$CN (1 : 1) with stirring at 60 °C to afford a clear solution within 6 h. The ^{1}H NMR spectrum of the *in situ* prepared sample (D$_2$O : CD$_3$CN (1 : 1), 298 K, *i.e.*, 25 °C) also showed a single set of slightly broad peaks (SI Fig. S12).

The reaction was then repeated in a similar manner in H$_2$O : CH$_3$CN (1 : 1) followed by evaporation and washing with CH$_3$CN to isolate the targeted self-assembled complex as an off-white solid. Stock solutions were prepared by dissolving the isolated solid in either D$_2$O or D$_2$O : CD$_3$CN (1 : 1); these solutions were used for ^{1}H NMR spectral study at 298 K, *i.e.*, 25 °C. The obtained spectra of the isolated samples very closely resembled the spectra of the *in situ* prepared samples in D$_2$O and D$_2$O : CD$_3$CN (1 : 1), respectively (SI Fig. S17 and S18). Comparison of the peak positions of the ensuing coordination cage with the free ligand could not be made due to insolubility of **L** in D$_2$O or D$_2$O : CD$_3$CN (1 : 1). However, a comparison of the ^{1}H NMR spectra of **L** in CDCl$_3$ and the isolated cage is shown in Fig. 3(i) and (ii).

We propose the formation of [Pd$_8$(tmeda)$_8$(**L**)$_4$](NO$_3$)$_{16}$, **H1·16NO$_3$** on the basis of geometrical considerations of the chosen metal and ligand components.[32–34] Slow conformational changes at room temperature are likely responsible for the broad peaks of **H1·16NO$_3$**. This could be due to restricted rotation of the pyridine units around the pyridine–biphenyl linkages imposed by the methyl groups of tmeda, which are located near the bound pyridine units. Thus, we used *cis*-Pd(en)(NO$_3$)$_2$ to prepare [Pd$_8$(en)$_8$(**L**)$_4$](NO$_3$)$_{16}$ (**H2·16NO$_3$**); the ^{1}H NMR spectrum of this complex in D$_2$O at room temperature (298 K, *i.e.*, 25 °C) showed sharp peaks (see SI Fig. S19). ^{1}H NMR spectra of **H1·16NO$_3$** were recorded at an elevated temperature (333 K, *i.e.*, 60 °C) in D$_2$O or D$_2$O : CD$_3$CN (1 : 1), and sharp peaks were obtained (see Fig. 3 and SI Fig. S18), indicating fast conformational changes at elevated temperature. In our prior experience, good crystals are more easily obtained when the *cis*-protecting group is tmeda rather than en; hence, we used **H1·16NO$_3$** for the planned host–guest interaction study.

Further NMR characterization, including ^{13}C, H–H COSY, NOESY, HSQC and DOSY, was carried out for **H1·16NO$_3$** in D$_2$O : CD$_3$CN (1 : 1) due to the better solubility in this mixed solvent, which allowed the possibility to obtain samples at higher concentration (see SI Fig. S21–S29). However, the host–guest study was performed in D$_2$O, keeping in mind the role of water as a universal solvent in biosystems. The ^{13}C NMR spectrum of the sample showed a single set of peaks even at room temperature, and DOSY showed a single diffusion band ($D = 1.77 \times 10^{-10}$ m^2 s^{-1}) for all the protons, thereby supporting the formation of a single discrete product. The ESI-MS study was not successful for **H1·16NO$_3$**; however, it was successful for the related complex [Pd$_8$(tmeda)$_8$(**L**)$_4$](PF$_6$)$_{16}$ (**H1·16PF$_6$**), which was prepared by adding NH$_4$PF$_6$ to a solution of **H1·16NO$_3$** in H$_2$O. The experimentally obtained isotopic pattern peaks at $m/z = 846.44$, 1045.11 and 1342.65 corresponding to the polycationic components [**M**–6PF$_6$]$^{6+}$, [**M**–5PF$_6$]$^{5+}$ and [**M**–4PF$_6$]$^{4+}$ were found
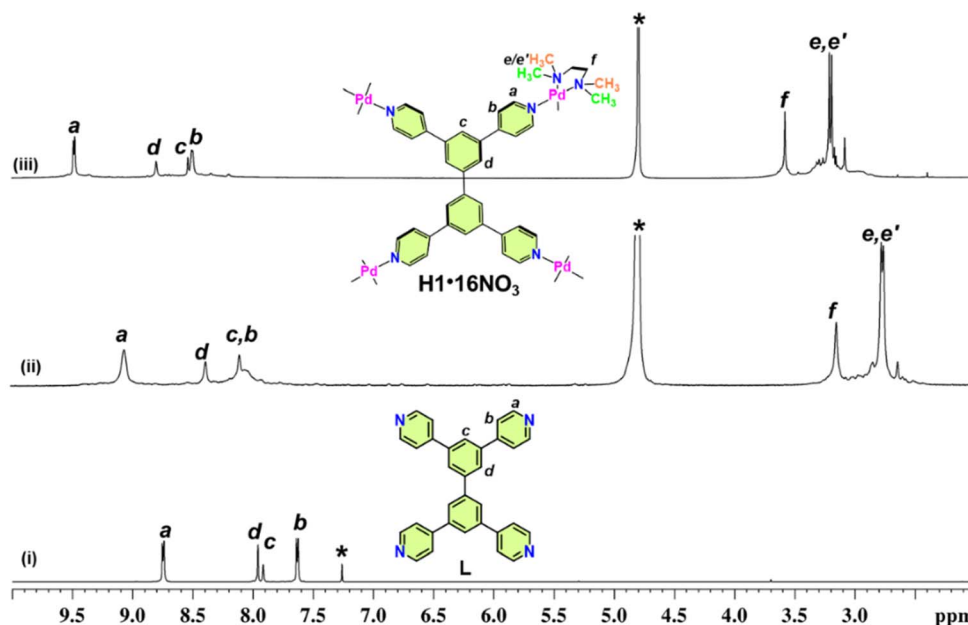

Fig. 3 400 MHz ^{1}H NMR spectra of (i) ligand **L** in CDCl$_3$ at 298 K, *i.e.*, 25 °C, and (ii and iii) isolated [Pd$_8$(tmeda)$_8$(L)$_4$](NO$_3$)$_{16}$, **H1·16NO$_3$** in D$_2$O at 298 K/333 K, *i.e.*, 25 °C/60 °C.

to be comparable with the simulated patterns, thus supporting the formation of the proposed octa-nuclear complexes (see SI Fig. S30 and S31).

Fortunately, we obtained good-quality crystals suitable for data collection *via* slow diffusion of 1,4-dioxane into a concentrated solution of **H1·16PF₆** in CH₃CN. The complex crystallized in the tetragonal space group $I4/m$. The asymmetric unit contains one-eighth of a molecule of the polycationic cage, which includes half of a molecule of ligand **L** coordinated to one Pd(II) center, four hexafluorophosphate anions (all half-occupancy, with one disordered by symmetry about a four-fold rotoinversion axis). The crystal structure (Fig. 2, see SI Section S6 for details) confirmed the proposed formula and revealed the relative arrangement of the ligand units in the molecular cuboid architecture [Pd₈(tmeda)₈(**L**)₄]¹⁶⁺.

The molecular cuboid **H1·16NO₃** is water-soluble and possesses a confined hydrophobic cavity that should be suitable for binding large hydrophobic guest molecules of suitable shapes/sizes. Thus, the hexadecacationic cuboid, *i.e.*, (**H1**)¹⁶⁺, is considered here as the potential H$_{out}$ type unit. A cartoon representation depicting the shape of the cationic cavity is shown in Fig. 4(A).

2.3 Ether podands and crown ethers: H$_{in}$ type hosts

The ether podands and crown ethers (**H3** to **H8**) evaluated in this work are shown in Fig. 4. The podands **H3** and **H4** are *ortho*-substituted benzene derivatives having a total of four and six oxygen donor sites, respectively, located on two symmetrical arms. Dibenzo[18]crown-6 (**H6**) is the first crown ether ring prepared by Pedersen that has two *ortho*-substituted benzene rings and six oxygen donor sites arranged in a cyclic array.[39] The crown ethers **H7** and **H8** are higher homologues having seven and eight oxygen donors, respectively. The macrocyclic rings **H5** and **H6** are of comparable size, but **H5** is less hydrophobic as it has only one aromatic ring. The host molecules **H3** to **H8** were considered as H$_{in}$, as we expected that they could enter the cavity of H$_{out}$ and still act as a host in this encapsulated form.

2.4 Cs⁺ ions as the guest G of the podands/crown ethers: [(G)⊂(H$_{in}$)$_x$]

Podands and crown ethers are known for the binding and extraction of alkali metal ions.[40,41] Typically, crown ethers are more efficient than podands; however, podands may enjoy a kinetic advantage over crown ethers. We were interested in exploiting the binding of the Cs⁺ ion by H$_{in}$ type hosts inside the cavity of an H$_{out}$ type host in water. The binding of commercially available Cs⁺ in water is of immense importance, as Cs⁺ is a surrogate of the hazardous radionuclides ¹³⁴Cs and ¹³⁷Cs that are produced as the main nuclear waste of the uranium fission reaction.[42] Crystal structures[43,44] have been reported for [(Cs)⊂(**H6**)₂]⁺, in which the ratio of host to guest is 2 : 1. The larger crown ethers **H7** and **H8** are known to bind Cs⁺ to form [(Cs)⊂(dibenzo[21]crown-7)(X)]⁺ and [(Cs)⊂(dibenzo[24]crown-8)(X)]⁺, where X represents additional coordination sites provided by suitable additives.[45,46] We believed that one or more units of **H6** might become encapsulated in the cavity of (**H1**)¹⁶⁺, and that the encapsulated crown ether would still retain its host-like ability for capturing alkali metal ions. In view of the above-mentioned 2 : 1 binding mode and the availability of space inside the cavity of H$_{out}$ for hosting [(Cs)⊂(**H6**)₂]⁺, it should be possible to generate a [{(G)⊂(H$_{in}$)₂}⊂(H$_{out}$)] type entity in which Cs⁺ is securely lodged as a guest and encapsulated by multiple layers. In this context, we wished to evaluate the hosting behaviour of the podands and the larger crown ethers when encapsulated inside H$_{out}$.

2.5 A typical host H$_{in}$ as the guest of a super-host H$_{out}$: [(H$_{in}$)$_x$⊂(H$_{out}$)]

Before proceeding to the synthesis of the targeted [{(G)⊂(H$_{in}$)₂}⊂(H$_{out}$)] type assembly, we decided to study the hosting abilities of (**H1**)¹⁶⁺, *i.e.*, H$_{out}$, towards the podands/crown ethers (**H3** to **H8**). The podands **H3** and **H4** are water soluble, as is the crown ether **H5**. However, the crown ethers **H6**, **H7** and **H8** are not soluble in water. The encapsulation study was performed by portion-wise addition of a variety of water-soluble H$_{in}$ (*i.e.*, **H3** to **H5**) to a solution of H$_{out}$ (*i.e.*, **H1·16NO₃**) in D₂O, and the
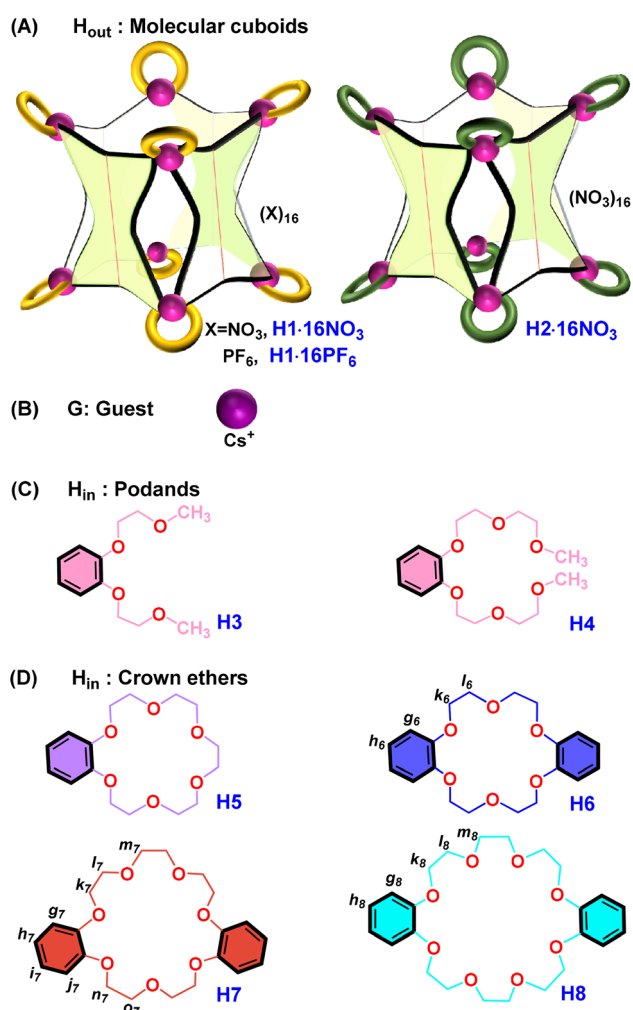

Fig. 4 (A) Cuboid-shaped self-assembled coordination cages as H$_{out}$. (B) Spherical monoatomic alkali metal ion Cs⁺ as G. (C and D) Selected podands and crown ethers as H$_{in}$.

progress of the reactions was followed by recording ^{1}H NMR spectra of the samples to evaluate the value of "x" in the probable $[(H_{in})_x \subset (H_{out})]$ type entities. The water-soluble podands **H3** and **H4** could be encapsulated by $(H1)^{16+}$, as can be seen from the shift of the signals observed in the ^{1}H NMR spectra recorded during the monitoring (see SI Fig. S35 and S36). However, changes in the peak positions could be seen even after the addition of several equivalents of the podands. The formation of $[(H3)_x \subset (H1)] \cdot 16NO_3$ (**1**) and $[(H4)_x \subset (H1)] \cdot 16NO_3$ (**2**) is proposed, although the value of "x" could not be deduced. This situation was also observed for the binding of water-soluble crown ether **H5** (see SI Fig. S37), for which the value of x in $[(H5)_x \subset (H1)] \cdot 16NO_3$ (**3**) could not be calculated.

An excess amount of each water-insoluble H_{in} (*i.e.*, **H6**, **H7** or **H8**) was added to a solution of H_{out} (*i.e.*, **H1·16NO$_3$**) in D$_2$O, and the reaction mixture was stirred at room temperature for 12 h. The mixture was then centrifuged, and the supernatant was evaporated to isolate the ensuing $[(H_{in})_x \subset (H_{out})]$ type assemblies. We propose that the cavity of $(H1)^{16+}$ accommodated two units of crown ethers in D$_2$O, resulting in $[(H6)_2 \subset (H1)] \cdot 16NO_3$ (**4**), $[(H7)_2 \subset (H1)] \cdot 16NO_3$ (**5**) and $[(H8)_2 \subset (H1)] \cdot 16NO_3$ (**6**) (Fig. 5, step (i) and step (ii); SI Fig. S117, step (ii)). This binding stoichiometry, *i.e.*, $x = 2$, is proposed based on the calculated integration ratios of the signals related to H_{out} and encapsulated H_{in} in the ^{1}H NMR spectra of isolated samples recorded in D$_2$O (see Fig. S38–S40).

Proton d of $(H1)^{16+}$ shows a remarkable upfield shift upon uptake of the crown ethers (compare Fig. 6(i) with Fig. 6(ii), (iv) and (vi) for uptake of **H6**, **H7** and **H8**, respectively) indicating its location above the plane of the aromatic rings of the encapsulated crown ethers. This effect is especially pronounced in the case of **H6** (compare Fig. 6(i) with Fig. 6(ii)), indicating restricted movement of **H6** in the cavity. In addition to ^{1}H NMR, compounds **4**, **5** and **6** were also characterised using various NMR spectroscopic techniques including ^{13}C, COSY, HSQC, and NOESY (see SI Fig. S41–S72). The DOSY NMR data for compounds **4**, **5** and **6** (see Fig. S73–S75) supports the encapsulation of the dibenzo-crown ethers (H_{in}) in the cavity of the molecular cuboid (H_{out}), as all signals for all of these compounds present as a single diffusion band.

To determine whether the molecular cuboid had any preference for the binding of a particular crown ether over another, we conducted competition experiments and recorded the corresponding ^{1}H NMR spectra. Addition of **H7** to a solution of $[(H6)_2 \subset (H1)] \cdot 16NO_3$ (**4**) in D$_2$O resulted in the formation of $[(H7)_2 \subset (H1)] \cdot 16NO_3$ (**5**) (Fig. 5, step (vii) and SI Fig. S76), whereas addition of **H6** to a solution of **5** in D$_2$O resulted in no changes. This data suggested the preferential binding of **H7** over **H6** by $(H1)^{16+}$. Similar experiments revealed that the binding of **H8** was preferred over that of **H6** (see SI Fig. S117, step (vii) and Fig. S77). However, addition of **H8** to a D$_2$O solution of **5** or addition of **H7** to a D$_2$O solution of **6** resulted in the formation of a mixture of products, as observed in their ^{1}H NMR spectra. We believe that the host $(H1)^{16+}$ does not favour the binding of **H7** over **H8** or *vice versa* (see SI Fig. S118, step (vii) and (viii), and Fig. S78). This lack of competition possibly generates multiple compounds including $[(H7)(H8) \subset (H1)] \cdot 16NO_3$ (**7**). Thus, the affinity is proposed to follow the order **H8** $\approx$ **H7** > **H6**.

2.6 Host–guest complex $[(G) \subset (H_{in})_2]$ as the guest of the super-host H_{out}: $[\{(G)(H_{in})_2\} \subset (H_{out})]$

Since **H6** is known to form a $[Cs \subset (H6)_2]^+$ type complex, we anticipated the formation of $[\{(Cs) \subset (H6)_2\} \subset (H1)] \cdot 17NO_3$ (**8**) *via* the direct addition of excess CsNO$_3$ to a solution of $[(H6)_2 \subset (H1)] \cdot 16NO_3$ (Fig. 5, step (iii)) or one-pot mixing of an excess of CsNO$_3$, an excess of **H6** and $(H1) \cdot 16NO_3$ in D$_2$O (Fig. 5, step (v)). The ^{1}H NMR spectra of the resulting assembly (proposed as **8**) prepared by either method were found to be comparable. The spectrum of resulting assembly **8** is shown in Fig. 6(iii); it revealed the retention of 2 units of encapsulated **H6** and an appreciable downfield/upfield shift of the aromatic/aliphatic proton signals of the **H6** moiety compared to those in the spectrum of **4** (compare Fig. 6(iii) with Fig. 6(ii)). Interestingly, the geminal methylene protons of **H6** (geminal protons k_6, as well as l_6) were found to be non-equivalent. Additionally, the *para*-substituted pyridine rings of coordinated **L** in **8** showed four signals instead of the expected two signals. These observations suggest unsymmetrical environments for these protons due to the restricted rotation of the pyridyl groups with respect to the biphenyl core and the restricted rotation of the ethylene spacers of the **H6** units in the structure of **8**, as shown

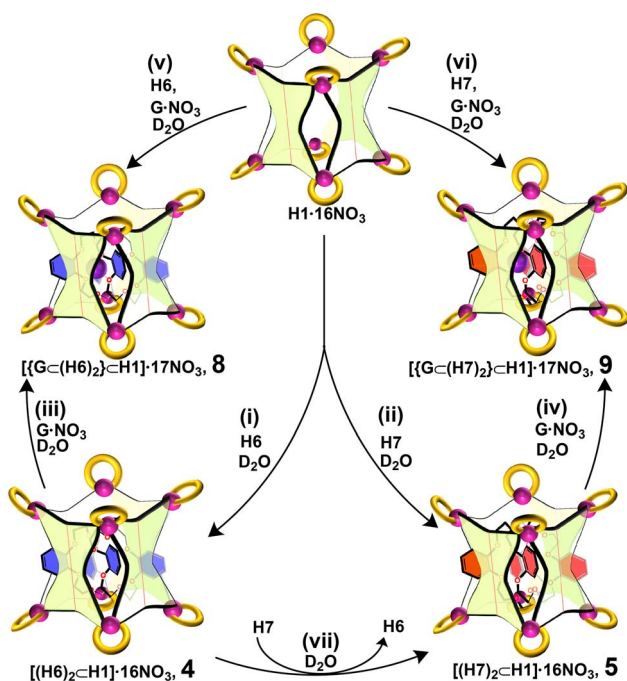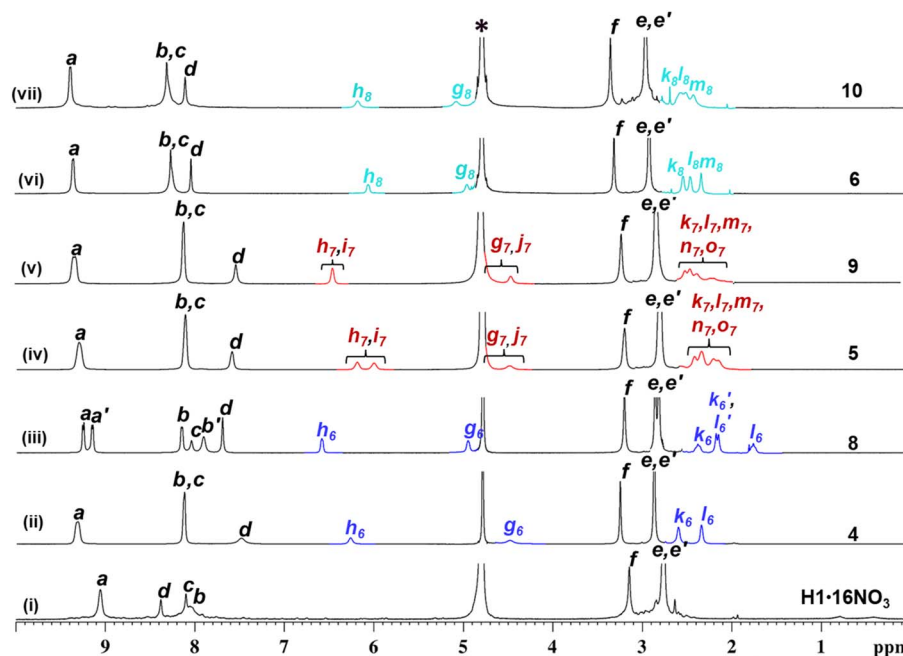**Fig. 5** Designer coordination cage $(H1)^{16+}$ as super-host H_{out} for encapsulation of (i and ii) two units of typical crown ethers (**H6**/**H7**) as H_{in} to form $[(H_{in})_2 \subset (H_{out})]$. (iii and iv) Addition of Cs$^+$ as G after accommodation of the two units of crown ether to form $[\{(G) \subset (H_{in})_2\} \subset (H_{out})]$. (v and vi) Combination of one equivalent of Cs$^+$ ions and two equivalents of typical crown ethers in a single pot to form $[\{(G) \subset (H_{in})_2\} \subset (H_{out})]$. (vii) Encapsulation of one crown ether over another in a selective manner, showing the preference for **H7** over **H6** (the behaviour of **H8** is found to be comparable with that of **H7**).

Fig. 6 ¹H NMR spectra (400 MHz, D₂O, 298 K, *i.e.*, 25 °C) for isolated samples of (i) **H1·16NO₃**, (ii) [(H6)₂⊂H1]·16NO₃ (**4**), (iii) [{G⊂(H6)₂}⊂H1]·17NO₃ (**8**), (iv) [(H7)₂⊂H1]·16NO₃ (**5**), (v) [{G⊂(H7)₂}⊂H1]·17NO₃ (**9**), (vi) [(H8)₂⊂H1]·16NO₃ (**6**), and (vii) [{G⊂(H8)₂}⊂H1]·17NO₃ (**10**).

in Fig. 7(A). This proposal is also supported by the COSY and NOESY data (Fig. 7(B) and (C)). The NOESY data for **8** reveals cross-peak correlations between the aromatic proton g₆ and the

aliphatic protons k₆, k₆′, l₆ and l₆′; however, no such correlations are observed between the aromatic proton h6 and the aliphatic protons (Fig. 7(B)). The ¹³³Cs NMR spectrum of a sample
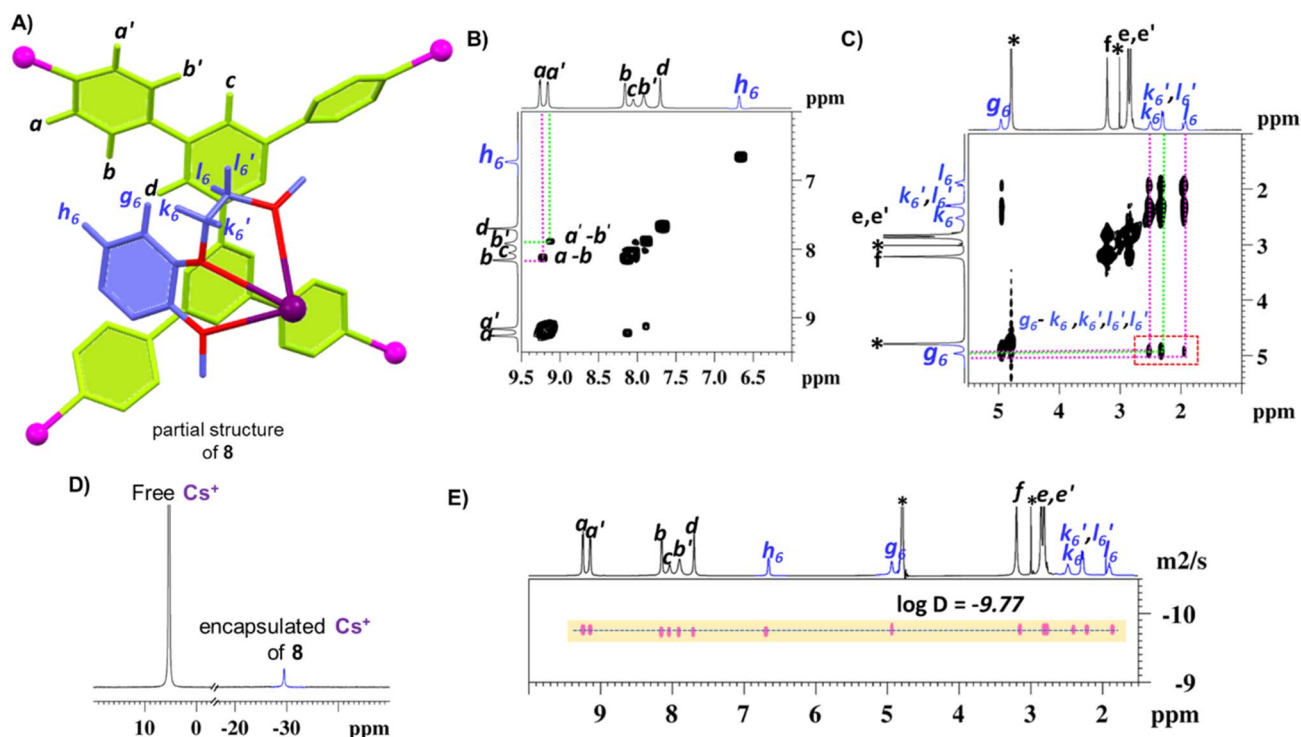

Fig. 7 (A) Partial representation of [{G⊂(H6)₂}⊂H1]·17NO₃, **8**, showing one of the walls of the super-host and part of the encapsulated host–guest complex. (B and C) Partial ¹H–¹H COSY and ¹H–¹H NOE spectra (400 MHz, D₂O, 298 K) emphasising correlations between certain protons (for COSY: a with b and a′ with b′; for NOE: g₆ with k₆, k₆′, l₆, and l₆) for characterization of **8**. (D) ¹³³Cs NMR spectrum (66 MHz, D₂O, 298 K) of **8** in the presence of excess Cs⁺, supporting the encapsulation of G, *i.e.*, Cs⁺. (E) ¹H-DOSY NMR spectrum (500 MHz, D₂O, 298 K) of **8** showing a single band for which the calculated diffusion coefficient (*D*) value is 1.67 × 10⁻¹⁰ m² s⁻¹.

containing a tenfold excess of Cs$^+$ showed an upfield-shifted signal for the bound Cs$^+$ present in compound **8** (Δδ of ~35 ppm) compared to the signal of free Cs$^+$ as shown in Fig. 7(D), confirming the presence of a well-shielded Cs$^+$. The single diffusion band in the DOSY spectrum of **8** supported the existence of only one product (Fig. 7(E)). On the basis of the ^{1}H NMR spectrum, we propose that the conformational changes in the backbone of **H6** are highly restricted, as it wraps around Cs$^+$ and is located in the cavity of (**H1**)$^{16+}$. It is likely that all the oxygen atoms of **H6** are coordinated with Cs$^+$, resulting in restricted rotation.

The compounds [{(Cs)(H7)$_2$}⊂(H1)]·17NO$_3$ (**9**) and [{(Cs)(H8)$_2$}⊂(H1)]·17NO$_3$ (**10**) were prepared in a manner very similar to **8**. The aromatic protons of the **H7** moiety of **9** were reasonably downfield-shifted, whereas the aliphatic protons showed a marginal downfield shift and broadening as compared to those of **5** (compare Fig. 6(v) with Fig. 6(iv)). The aromatic/aliphatic protons of the **H8** moiety of **10** are

marginally downfield-shifted and broadened (compare Fig. 6(vii) with Fig. 6(vi)). The *para*-substituted pyridine rings of coordinated **L** in **9** and **10** showed only two signals in contrast to the four signals observed in the case of **8**. Thus, the conformational movement of the **L** moiety and the **H7/H8** moiety in complexes **9/10** is not restricted. It is likely that not all the oxygen atoms of **H7/H8** are coordinated with Cs$^+$ simultaneously, thus allowing conformational changes. The compounds **8**, **9** and **10** were characterised using various NMR spectroscopic techniques including ^{1}H, ^{13}C, COSY, NOESY and HSQC (see SI Fig. S80–S110). The DOSY NMR data for the compounds (see SI Fig. S111–S113) supports the formation of a single discrete product, as all the signals for all of these compounds belong to a single diffusion band. Stacked ^{1}H NMR spectra depicting the portion-wise addition of an aqueous solution of CsNO$_3$ to aqueous solutions of **4**, **5** and **6** to generate **8**, **9** and **10** are shown in SI Fig. S115–S117. For the binding of Cs$^+$ by the host-in-host system **4**, a slow guest-exchange was
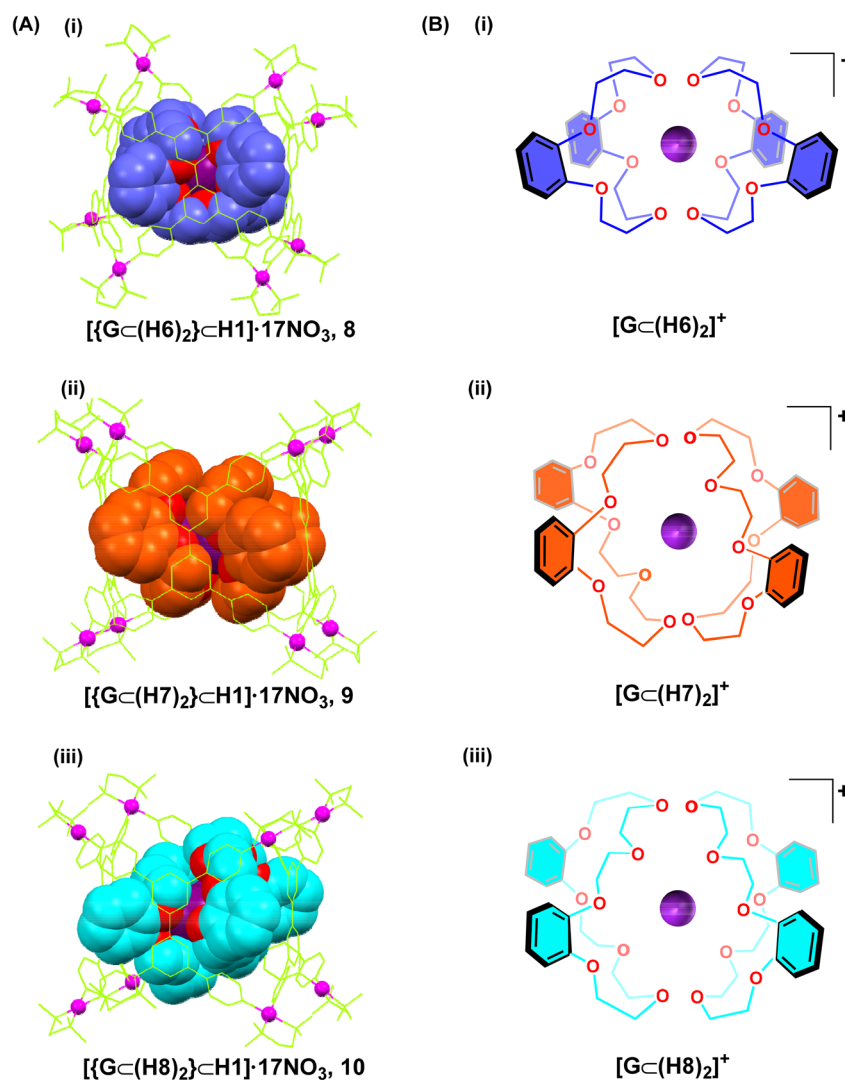

Fig. 8 (A) Crystal structures of **8**, **9** and **10** showing the super-host framework as a wireframe and the [Cs⊂(crown ether)$_2$]$^+$ as a space filling model. (B) Chemical drawings showing the relative orientation of the pair of encapsulated crown ether rings wrapped around Cs$^+$, *i.e.*, the [Cs⊂(crown ether)$_2$]$^+$ moieties as observed in the crystal structures of **8**, **9** and **10**.

observed and a high binding constant ($K_a > 10^5$ M^{-1}) is proposed,[47] as one equivalent of Cs^+ was sufficient to populate **4**. However, for the binding of Cs^+ by the host-in-host systems **5** and **6**, fast guest exchange was observed with a low binding constant in both cases; for the former case, K_a is approximately 10^2 M^{-1}, while for the latter case the value was too small to be estimated.

2.7 Crystal structures of $[\{(G)(H_{in})_2\} \subset (H_{out})]$ type complexes

We could not obtain suitable HRMS data for the $[\{(guest) \subset (host_{in})_2\} \subset (host_{out})]$ type molecules, but single-crystal X-ray crystallographic analysis unequivocally supported the formation of **8**, **9** and **10** (Fig. 8(A), see SI Section S6 for details). Single crystals were obtained by slow evaporation of their aqueous solutions at room temperature over a period of 3 weeks. Compound **8** crystallized in the tetragonal crystal system with the $I4_1/a$ space group. The asymmetric unit of **8** comprises one unit of ligand **L** coordinated to two units of *cis*-protected Pd(II) ions and half a molecule of the crown ether coordinated to a Cs^+ ion, which lies on the fourfold rotoinversion axis. Two nitrate ions were located and refined, one of which is disordered over three positions. In contrast, compounds **9** and **10** crystallized in the triclinic space group $P\bar{1}$. In case of **9**, the asymmetric unit contains half the complex, which includes two units of ligand **L** coordinated to four units of *cis*-protected Pd(II), five nitrate anions (four with full occupancy and one with half occupancy, which is disordered by symmetry), and one crown ether molecule coordinated to a Cs atom disordered over three positions (with occupancies of 0.15, 0.15 and 0.21). In the case of **10**, the asymmetric unit contains half the complex, which includes two units of the ligand **L** coordinated to four units of *cis*-protected Pd(II), six nitrate anions (five with full occupancy and one with half occupancy, which is disordered by symmetry), and one crown ether molecule coordinated to a Cs atom disordered over two positions (with occupancies of 0.15 and 0.08). The crystal structures of **8**, **9** and **10** confirm the inclusion of the caesium cation in the cavity of the cationic molecular cuboid; the electrostatic repulsion between the cationic entities is minimized by the three-dimensional screening of the Cs^+ ion by the two crown ether units (see Fig. 8). It is relevant here to look again at the architecture of the free cage $(H1)^{16+}$ through its crystal structure (Fig. 2) and cartoon depiction (Fig. 4). In the architecture of $(H1)^{16+}$, there are two square-shaped open windows, one at the top and the other at the bottom of the cuboid-cage, each of which is demarcated by the four Pd(II) units. Additionally, there are four narrow slits located along the edges of the cuboid, vertically located between the square windows, with each being demarcated by two units of Pd(II). There are four phenylene units from the two units of encapsulated dibenzo crown ether molecules per cuboid cage, as shown in the crystal structures of **8**, **9** and **10**. In all cases, these four phenylene units are located in the four narrow slits of the cuboid, with one in each slit. The ethylene-oxide units of the crown ether are located at the core of the cuboid, and the oxygen atoms are pointed approximately towards the centre of the cuboid, interacting with the deeply confined Cs^+ ion. The overall structures of the encapsulated

$[(Cs) \subset (crown\ ether)_2]^+$ complexes are shown in a simplified manner in Fig. 8(B) for clarity, although there is disorder in the crystal structures.

2.8 Adaptive deformation of the super-host H_{out}

The stimulus-induced adaptive deformation of coordination architectures, in line with enzymatic behaviour, is a subject of contemporary interest.[48–50] A selective stimulus-induced adaptive deformation of the molecular cuboid super-host is observed in this work, where the unique stimulus is a specific host–guest complex, *i.e.*, $[(Cs) \subset (H6)_2]^+$. This finding can be described by comparing the initial structure of $(H1)^{16+}$ and the deformed structure $[\{(Cs) \subset (H6)_2\} \subset (H1)]^{17+}$ as depicted in Fig. 9 in cartoon format.

The dimensions of both the square-shaped open windows of the Pd_8L_4 type cuboid $(H1)^{16+}$ described by the four co-planar metal centres are 13.40×13.40 Å, with bisecting diagonals of 18.95 Å. The remaining four ligand-panelled walls of $(H1)^{16+}$ are rectangular-shaped and are described by the four metal centres, having dimensions of 13.40×11.78 Å with bisecting diagonals of 17.84 Å in each case. The cuboid architecture of $(H1)^{16+}$ became deformed upon the encapsulation of $[(Cs) \subset (H6)_2]^+$ to form the cationic part of the compound **8**; the four metal centres, which are not co-planar, of both the open windows described a puckered rhombus with arms of 13.33×13.34 Å and non-bisecting diagonals of unequal lengths, namely, 21.89 and 14.04 Å. The adjacent bond angles of the rhombus are 110° and 63°, respectively. Further, the pair of puckered open windows are located in a staggered configuration with respect to each other. The four panelled walls of compound **8** are also mildly puckered, having rectangular dimensions of 13.33/13.34 $\times$ 12.25 Å and non-intersecting diagonals of 17.63 and 17.73 Å, respectively. However, no deformation was observed due to uptake of either $[(Cs) \subset (H7)_2]^+$ or $[(Cs) \subset (H8)_2]^+$ by $(H1)^{16+}$ to form the cationic parts of **9** and **10**, respectively.
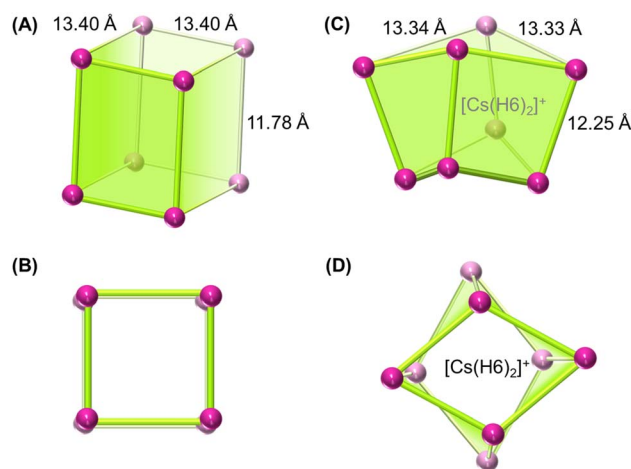

Fig. 9 Cartoon representations for comparison of the architectures of (A and B) cuboid-shaped $[H1]^{16+}$ and (C and D) the deformed cuboid in $[\{Cs \subset (H6)_2\} \subset H1]^{17+}$ as viewed from the side and top.

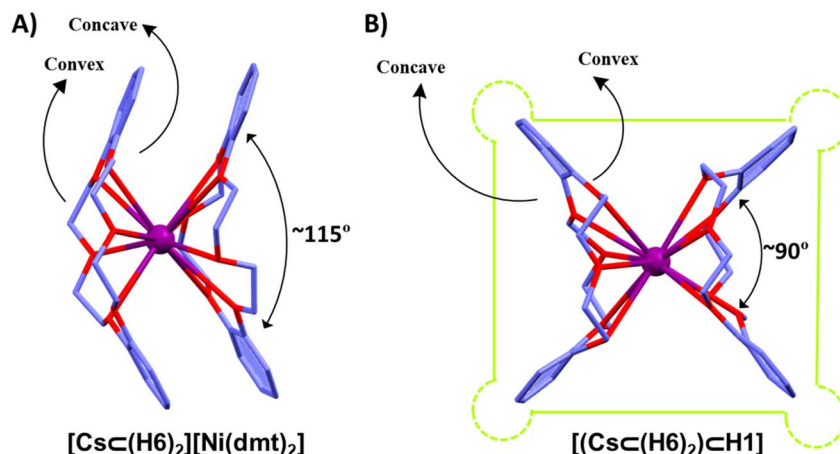**Fig. 10** Structural comparison of $[Cs \subset (H6)_2]^+$ when (A) exists in its native state (reported work) and (B) encapsulated in the molecular cuboid (this work).

2.9 Structure of $[(Cs) \subset (H6)_2]^+$ in native and encapsulated forms

A comparison of the solid-state structure of $[(Cs) \subset (H6)_2]^+$ in its native form[43] with that in its encapsulated form revealed interesting conformational details, as shown in Fig. 10. The caesium atom is sandwiched between two **H6** molecules in each case, and the crown ether is not flat but bowl-shaped. In the native state, one unit of **H6** provides its convex face and the other provides its concave face for coordination with caesium (Fig. 10(A)). However, in the encapsulated state, both crown ether units provide their convex face for binding caesium (Fig. 10(B)). The structural change in $[(Cs) \subset (H6)_2]^+$ after being encapsulated as a guest by H_{out} is due to $\pi \cdots \pi$ and $C-H \cdots \pi$ interactions between the protons of **H6** and the aromatic rings of the ligand in **H1**. The planes of the two phenylene rings of a crown ether unit in the native and encapsulated states are disposed in a divergent manner, subtending dihedral angles of $\sim 115°$ and $90°$, respectively. This observation suggests that the molecular cuboid induces bending of the guest (**H6**) by $\sim 25°$ to fit into the cavity.

3 Conclusions

In summary, we have successfully synthesized a new water-soluble template-free polycationic molecular cuboid. The molecular cuboid (H_{out}) encapsulates selected crown ether molecules (H_{in}) in its nano-confinement, providing a family of host-in-host type complexes of the type $[(H_{in})_2 \subset (H_{out})]$. Preferential binding of certain crown ethers over others is demonstrated in these complexes. Encapsulation of the caesium ion (G) at the centre of the host-in-host complex resulted in $[\{(G) \subset (H_{in})_2\} \subset (H_{out})]$ type molecules in which a cationic guest is accommodated in a cationic host due to the screening effect provided by the crown ether units. From another view-point, host–guest complexes of suitable shapes/sizes are recognized in larger host molecules. This finding encourages the binding study of small-sized hosts, and host–guest complexes in the cavity of large-sized host molecules to prepare ensembles that are expected to exhibit a variety of novel behaviours.

Author contributions

D. K. C. and M. R. conceptualized the idea, carried out the research, analysed the data and wrote the manuscript. S. K. carried out X-ray diffraction experiments and refined the crystal structures and contributed to the manuscript preparation. D. K. C. is the principal investigator and managed the project.

Conflicts of interest

There are no conflicts to declare.

Data availability

Acknowledgements

References

1 G. W. Gokel, W. M. Leevy and M. E. Weber, *Chem. Rev.*, 2004, **104**, 2723–2750.

2 G. Montà-González, F. Sancenón, R. Martínez-Máñez and V. Martí-Centelles, *Chem. Rev.*, 2022, **122**, 13636–13708.

3 E. G. Percástegui, T. K. Ronson and J. R. Nitschke, *Chem. Rev.*, 2020, **120**, 13480–13544.

4 H. Takezawa and M. Fujita, *Bull. Chem. Soc. Jpn.*, 2021, **94**, 2351–2369.

5 R. Banerjee, D. Chakraborty and P. S. Mukherjee, *J. Am. Chem. Soc.*, 2023, **145**, 7692–7711.

6 Y. Sun, C. Chen, J. Liu and P. J. Stang, *Chem. Rev.*, 2020, **49**, 3889–3919.

7 M. Yoshizawa and L. Catti, *Acc. Chem. Res.*, 2019, **52**, 2392–2404.

8 C. J. T. Cox, J. Hale, P. Molinska and J. E. M. Lewis, *Chem. Soc. Rev.*, 2024, **53**, 10380–10408.

9 L. Escobar and P. Ballester, *Chem. Rev.*, 2021, **121**, 2445–2514.

10 K. Lizuka, H. Takezawa and M. Fujita, *J. Am. Chem. Soc.*, 2023, **145**, 25971–25975.

11 K. Lizuka, H. Takezawa and M. Fujita, *J. Am. Chem. Soc.*, 2024, **146**, 32311–32316.

12 L. Neira, C. Alvariño, O. Domarco, B. Blanco, C. Peinador, M. D. García and J. M. Quintela, *Chem.–Eur. J.*, 2019, **25**, 14834–14842.

13 Y.-H. Huang, Y.-L. Lu, Z.-M. Cao, X.-D. Zhang, C.-H. Liu, H.-S. Xu and C.-Y. Su, *J. Am. Chem. Soc.*, 2024, **146**, 21677–21688.

14 A. I. Day, R. J. Blanch, A. P. Arnold, S. Lorenzo, G. R. Lewis and I. A. Dance, *Angew. Chem., Int. Ed.*, 2002, **41**, 275–277.

15 T. Kawase, Y. Nishiyama, K. Nakamura, T. Ebi, K. Matsumato, H. Kurata and M. Oda, *Angew. Chem., Int. Ed.*, 2007, **46**, 1086–1088.

16 Y. Xia, Y. Jiang, X.-L. Ni, Q. Wang and D. A. Wang, *Chin. Chem. Lett.*, 2024, **35**, 109782.

17 T. Kawase, K. Tanaka, N. Shiono, Y. Seirai and M. Oda, *Angew. Chem., Int. Ed.*, 2004, **43**, 1722–1724.

18 H. Ueno, T. Nishihara, Y. Segawa and K. Itami, *Angew. Chem., Int. Ed.*, 2015, **54**, 3707–3711.

19 S.-Y. Kim, I.-S. Jung, E. Lee, J. Kim, S. Sakamoto, K. Yamaguchi and K. Kim, *Angew. Chem., Int. Ed.*, 2001, **40**, 2119–2121.

20 W. Gong, X. Yang, P. Y. Zavalij, L. Isaacs, Z. Zhao and S. Liu, *Chem.–Eur. J.*, 2016, **22**, 17612–17618.

21 K. Cai, M. C. Lipke, Z. Liu, J. Nelson, T. Cheng, Y. Shi, C. Cheng, D. Shen, J.-M. Han, S. Vemuri, Y. Feng, C. L. Stern, W. A. Goddard III, M. R. Wasielewski and J. F. Stoddart, *Nat. Commun.*, 2018, **9**, 5275.

22 S. Guo, L. Liu, F. Su, H. Yang, G. Liu, Y. Fan, J. He, Z. Lian, X. Li, W. Guo, X. Chen and H. Jiang, *JACS Au*, 2024, **4**, 402–410.

23 X.-Y. Pang, H. Zhou, X. Xie, W. Jiang, Y. Yang, J. L. Sessler and H.-Y. Gong, *Angew. Chem., Int. Ed.*, 2024, **63**, e202407805.

24 H. Danjo, Y. Hashimoto, Y. Kidena, A. Nogamine, K. Katagiri, M. Kawahata, T. Miyazawa and K. Yamaguchi, *Org. Lett.*, 2015, **17**, 2154–2157.

25 J. Jian, *Chem. Res. Chin. Univ.*, 2022, **38**, 407–409.

26 T. N. Parac, M. Scherer and K. N. Raymond, *Angew. Chem., Int. Ed.*, 2000, **39**, 1239–1242.

27 D. Zhang, T. K. Ranson, J. L. Greenfield, T. Brotin, P. Berthault, E. Léonce, J.-L. Zhu, L. Xu and J. R. Nitschke, *J. Am. Chem. Soc.*, 2019, **141**, 8339–8345.

28 T. Sawada, H. Hisada and M. Fujita, *J. Am. Chem. Soc.*, 2014, **136**, 4449–4451.

29 E. Ubasart, O. Borodin, C. Fuertes-Espinosa, Y. Xu, C. García-Simón, L. Gómez, J. Juanhuix, F. Gándaram, I. Imaz, D. Maspoch, M. von Delius and X. Ribas, *Nat. Chem.*, 2021, **13**, 420–427.

30 C. Falaise, S. Khlifi, P. Bauduin, P. Schmid, W. Shepard, A. A. Ivanov, M. N. Sokolov, M. A. Shestopalov, P. A. Abramov, S. Cordier, J. Marrot, M. Haousa and E. Cadot, *Angew. Chem., Int. Ed.*, 2021, **60**, 14146–14153.

31 K. Lizuka, H. Takezawa and M. Fujita, *Angew. Chem., Int. Ed.*, 2025, **64**, e202422143.

32 R. Saha, A. Devaraj, S. Bhattacharyya, S. Das, E. Zangrando and P. S. Mukherjee, *J. Am. Chem. Soc.*, 2019, **141**, 8638–8645.

33 I. A. Bhat, R. Jain, M. M. Siddique, D. K. Saini and P. S. Mukherjee, *Inorg. Chem.*, 2017, **56**, 5352–5360.

34 P. Howlader, B. Mondal, P. C. Purba, E. Zangrando and P. S. Mukherjee, *J. Am. Chem. Soc.*, 2018, **140**, 7952–7960.

35 Y. Yamanoi, Y. Sakamoto, T. Kusukawa, M. Fujita, S. Sakamoto and K. Yamaguchi, *J. Am. Chem. Soc.*, 2001, **123**, 980–981.

36 S. Sharma, M. Sarkar and D. K. Chand, *Chem. Commun.*, 2023, **59**, 535–554.

37 M. Ray, S. Krishnaswamy, A. K. Pradhan and D. K. Chand, *Chem. Mater.*, 2023, **35**, 6702–6712.

38 W. Liu, C. Bobbala, C. L. Stern, J. E. Hornick, Y. Liu, A. E. Enciso, E. A. Scott and J. F. Stoddart, *J. Am. Chem. Soc.*, 2020, **142**, 3165–3173.

39 C. J. Pedersen, *J. Am. Chem. Soc.*, 1967, **89**, 7017–7036.

40 M. Valente, S. F. Sousa, A. L. Magalhães, C. Freire and J. Solut, *Chem*, 2010, **39**, 1230–1242.

41 G. G. Talanova, N. S. A. Elkarim, R. E. Hanes, H.-S. Hwang, R. D. Rogers and R. A. Bartsch, *Anal. Chem.*, 1999, **71**, 672–677.

42 J. Wang and S. Zhuang, *Nucl. Eng. Technol.*, 2020, **52**, 328–336.

43 T. Akutagawa, K. Shitagami, M. Aonuma, S.-I. Noro and T. Nakamura, *Inorg. Chem.*, 2009, **48**, 4454–4461.

44 A. N. Chekhlov, *Russ. J. Coord. Chem.*, 2009, **35**, 222–225.

45 C. Yan, Z. Li, X.-Q. Xiao, N. Wei, Q. Lu and M. Kira, *Angew. Chem., Int. Ed.*, 2016, **55**, 1484–1487.

46 M. Hu, X. Wang, Y. Jiang and S. Li, *Inorg. Chem. Commun.*, 2007, **11**, 85–88.

47 P. Thordarson, *Chem. Soc. Rev.*, 2011, **40**, 1305–1323.

48 H. Xu, T. K. Ronson, A. W. H. Heard, P. C. P. Teeuwen, L. Schneider, P. Pracht, J. D. Thoburn, D. J. Wales and J. R. Nitschke, *Nat. Chem.*, 2025, **17**, 289–296.

49 H. Hou, Z. Jiang, Q. Chen, Q.-F. Sun and M. Hong, *CCS Chem.*, 2025, 7, DOI: 10.31635/ccschem.025.202505454.

50 S. S. Mishra, S. Krishnaswamy and D. K. Chand, *J. Am. Chem. Soc.*, 2024, **146**, 4473–4488.

51 (*a*) M. Ray, S. Krishnaswamy and D. K. Chand, CCDC 2423199: Experimental Crystal Structure Determination, 2025, DOI: 10.5517/ccdc.csd.cc2mbjq7; (*b*) M. Ray, S. Krishnaswamy and D. K. Chand, CCDC 2423200: Experimental Crystal Structure Determination, 2025, DOI: 10.5517/ccdc.csd.cc2mbjr8; (*c*) M. Ray, S. Krishnaswamy and D. K. Chand, CCDC 2423201: Experimental Crystal Structure Determination, 2025, DOI: 10.5517/ccdc.csd.cc2mbjs9; (*d*) M. Ray, S. Krishnaswamy and D. K. Chand, CCDC 2423283: Experimental Crystal Structure Determination, 2025, DOI: 10.5517/ccdc.csd.cc2mbmf1.